Electronic Supplementary Material (ESI) for Physical Chemistry Chemical Physics.


# ELECTRONIC SUPPORTING INFORMATION

## Stepwise Microhydration of Aromatic Amide Cations: Water Solvation Networks Revealed by Infrared Spectra of Acetanilide$^+$-$(H_2O)_n$ Clusters (n≤3)

Johanna Klyne,[a] Matthias Schmies,[a] Mitsuhiko Miyazaki,[a,b] Masaaki Fujii,[b] Otto Dopfer[a]*

[a] Institut für Optik und Atomare Physik, Technische Universität Berlin, Hardenbergstr. 36, 10623 Berlin, Germany

[b] Laboratory for Chemistry and Life Science, Institute of Innovative Research, Tokyo Institute of Technology, Yokohama 226-8503, Japan.

* Corresponding author: Fax: (+49) 30-31423018, E-Mail: dopfer@physik.tu-berlin.de

**Table S1.** Calculated and experimental proton donor stretch frequencies of the acidic NH group ($\nu_{NH}$ in $cm^{-1}$) and corresponding frequency red shifts ($\Delta\nu_{XH}$ in $cm^{-1}$) of H-bonded $AA^+$-L(NH) and $FA^+$-L(NH) clusters as well as proton affinities (PA, in kJ $mol^{-1}$) of the ligands (L=Ar, $N_2$, $H_2O$, and $(H_2O)_2$).

| A | Monomer | | L = He | | L = Ar | | L = $N_2$ | | L = $H_2O$ | | L = $(H_2O)_2$ | |
|---|---|---|---|---|---|---|---|---|---|---|---|---|
| PA | | | 178 | | 369 | | 494 | | 691 | | 808 | |
| | $\nu_{NH}$ exp | $\nu_{NH}$ calc | $\Delta\nu_{NH}$ exp | $\Delta\nu_{NH}$ calc | $\Delta\nu_{NH}$ exp | $\Delta\nu_{NH}$ calc | $\Delta\nu_{NH}$ exp | $\Delta\nu_{NH}$ calc | $\Delta\nu_{NH}$ exp | $\Delta\nu_{NH}$ calc | $\Delta\nu_{NH}$ exp | $\Delta\nu_{NH}$ calc |
| $AA^+$ | 3385 | 3385 | 0 | -2 | -12 | -45 | -30 | -61 | -215 | -246 | -461 | -396 |
| $FA^+$ | 3380 | 3381 | | | -15 | -30 | -35 | -70 | -350 | -296 | -592 | -471 |

**Figure S1.** Structures of neutral c-/t-AA and most stable isomers of t-AA-$H_2O$ calculated at the ωB97X-D/aug-cc-pVTZ level. Relevant structural, energetic, and vibrational parameters are listed in Table 2. Relative energies ($E_0$) and binding energies ($D_0$) are given in $cm^{-1}$, while intermolecular (red) and intramolecular N-H, C=O, and O-H (black) bond lengths are given in Å.

**Figure S2.** Structure of the t-$AA^+$-$H_2O$(NH)-Ar(π) isomer calculated at the ωB97X-D/aug-cc-pVTZ level. Relevant structural, energetic, and vibrational parameters are listed in Table 2. Binding energies ($D_0$) are given in $cm^{-1}$, while intermolecular (red) and intramolecular N-H, C=O, and O-H (black) bond lengths are given in Å.

**Figure S3.** IRPD spectra of $AA^+$-$H_2O$ and $AA^+$-$H_2O$-Ar in the X-H stretch range compared to linear IR absorption spectra of t-$AA^+$-$H_2O$(NH)(-Ar(π)), t-$AA^+$-$H_2O$(CO), and c-$AA^+$-$H_2O$(NH)(-Ar(π) calculated at the ωB97X-D/aug-cc-pVTZ level (Table 1). The dashed lines indicate the experimental frequencies of bare t-$AA^+$ ($\nu_{NH}$=3385 $cm^{-1}$) and $H_2O$ ($\nu^{a/s}_{OH}$=3756/3657 $cm^{-1}$). All computed spectra are drawn to the same intensity scale but the intensities of the bound $\nu_{NH}$ transition in the c-/t-$AA^+$-$H_2O$(NH) spectra are multiplied by 0.1.

**Figure S4.** REMPI-IR (IR dip) spectra of t-$AA^+$-$H_2O$(NH) and t-$AA^+$-$H_2O$(NH) generated by REMPI[3] compared to EI-IR (IRPD) spectra of $AA^+$-$H_2O$ and $AA^+$-$H_2O$-Ar employing the EI ion source.

**Figure S5.** IRPD spectra of $AA^+$-$H_2O$-L with L=Ar and $N_2$ in the fingerprint range (loss of L) compared to linear IR absorption spectra of c-/t-$AA^+$-$H_2O$(NH)(-Ar(π)) and c-/t-$AA^+$ calculated at the ωB97X-D/aug-cc-pVTZ level. The positions, widths, and vibrational and isomer assignments of the transitions observed are listed in Table 1. For comparison, the IRPD spectrum of $AA^+$-Ar with the labeling of the transitions is reproduced from Ref. 59.

**Figure S6.** Comparison of the IRPD spectrum of cold cationic $AA^+$-$H_2O$-Ar and the IR dip spectrum measured for neutral t-AA-$H_2O$(NH) and t-AA-$H_2O$(NH),[3] and their corresponding linear IR absorption spectra calculated at the ωB97X-D/aug-cc-pVTZ level.

**Figure S7.** Comparison of the IRPD spectra of $AA^+$-$L_n$ with L=He, Ar, $N_2$,[59] and $H_2O$ obtained in the X-H stretch range.

**Figure S8.** NBO charge distribution (in me) of t-$AA^{(+)}$ and c-$AA^{(+)}$ in the $S_0$ and $D_0$ state calculated at the ωB97X-D/aug-cc-pVTZ level.

# FIGURE S1

t-AA

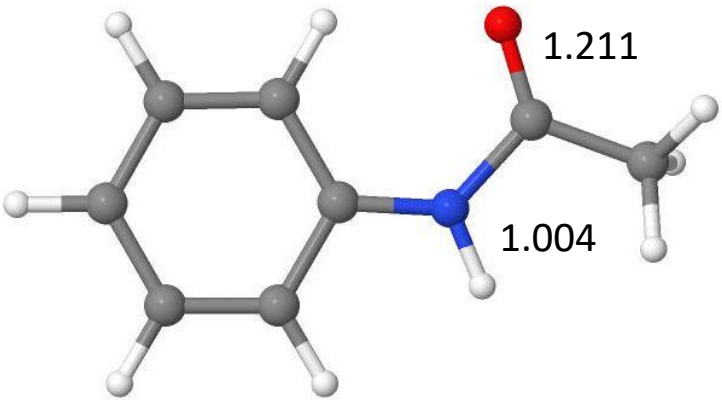


$E_0 = 0$

c-AA

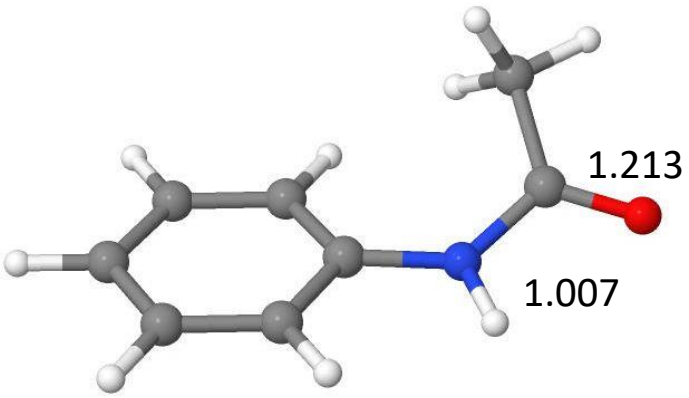


$E_0 = 694$

t-AA-$H_2O$(CO)

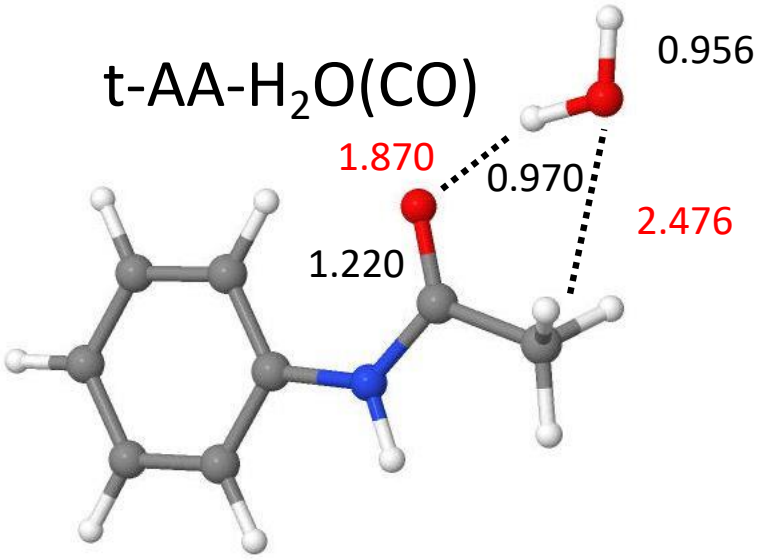


$D_0 = 1852$

t-AA-$H_2O$(NH)

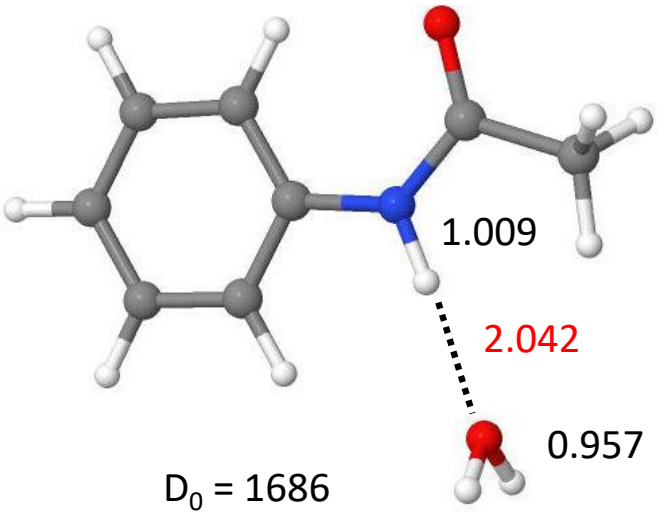


$D_0 = 1686$

t-AA-$H_2O$(CO-II)

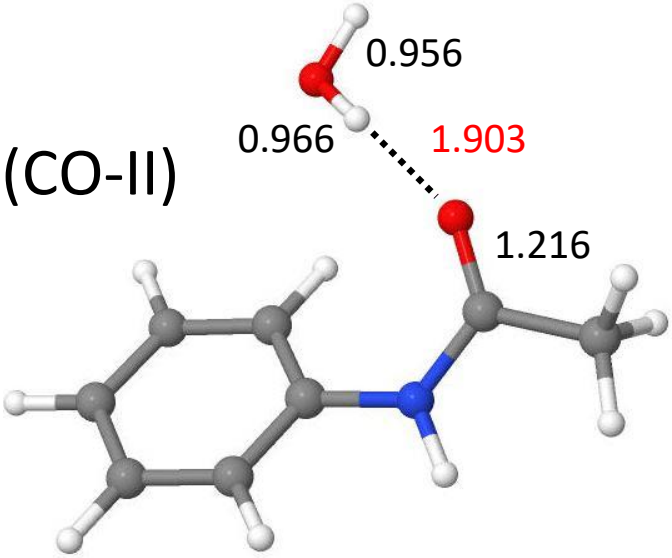


$D_0 = 1364$

t-AA$^{+}$-$H_2O$(NH)-Ar(π)

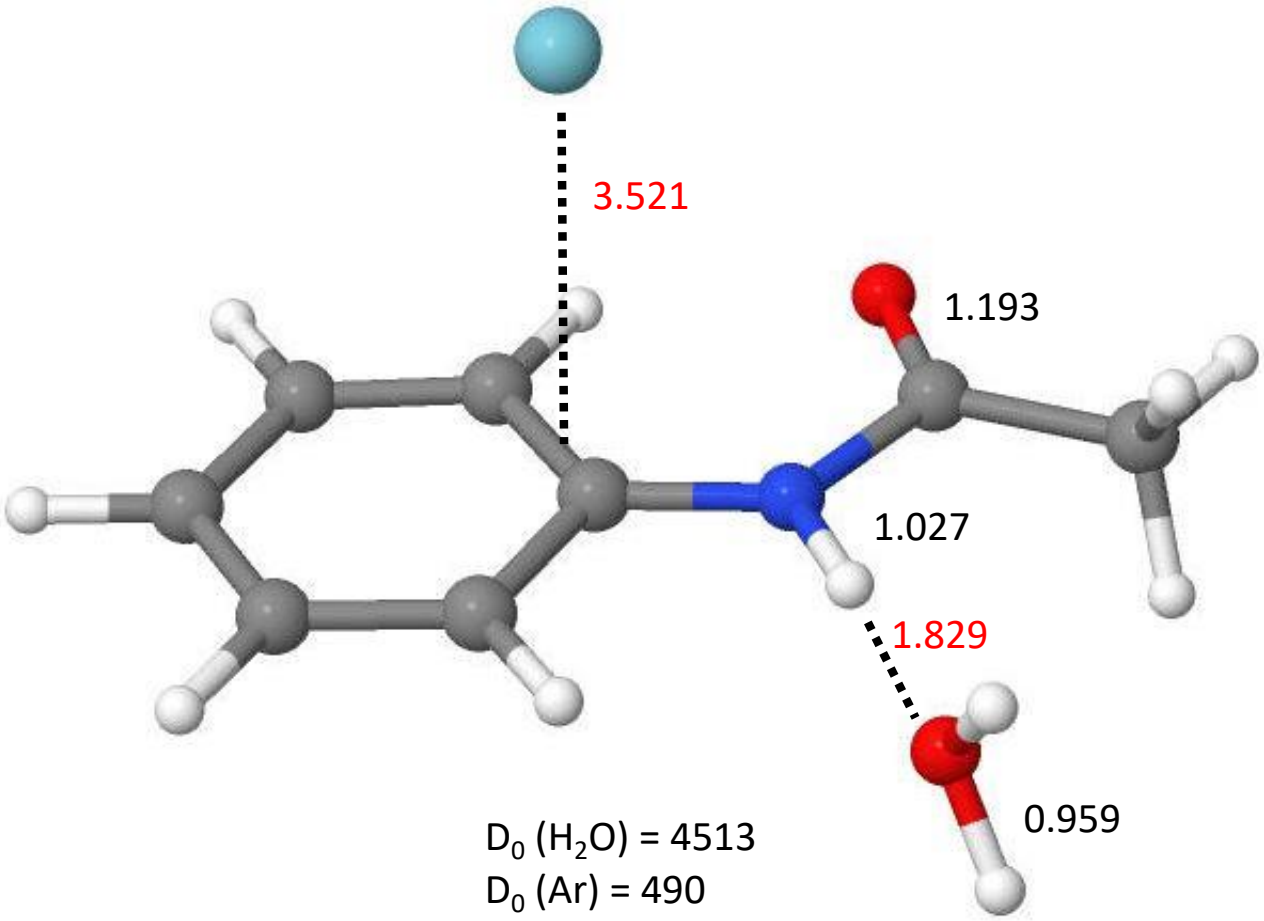


**FIGURE S2**

# FIGURE S3

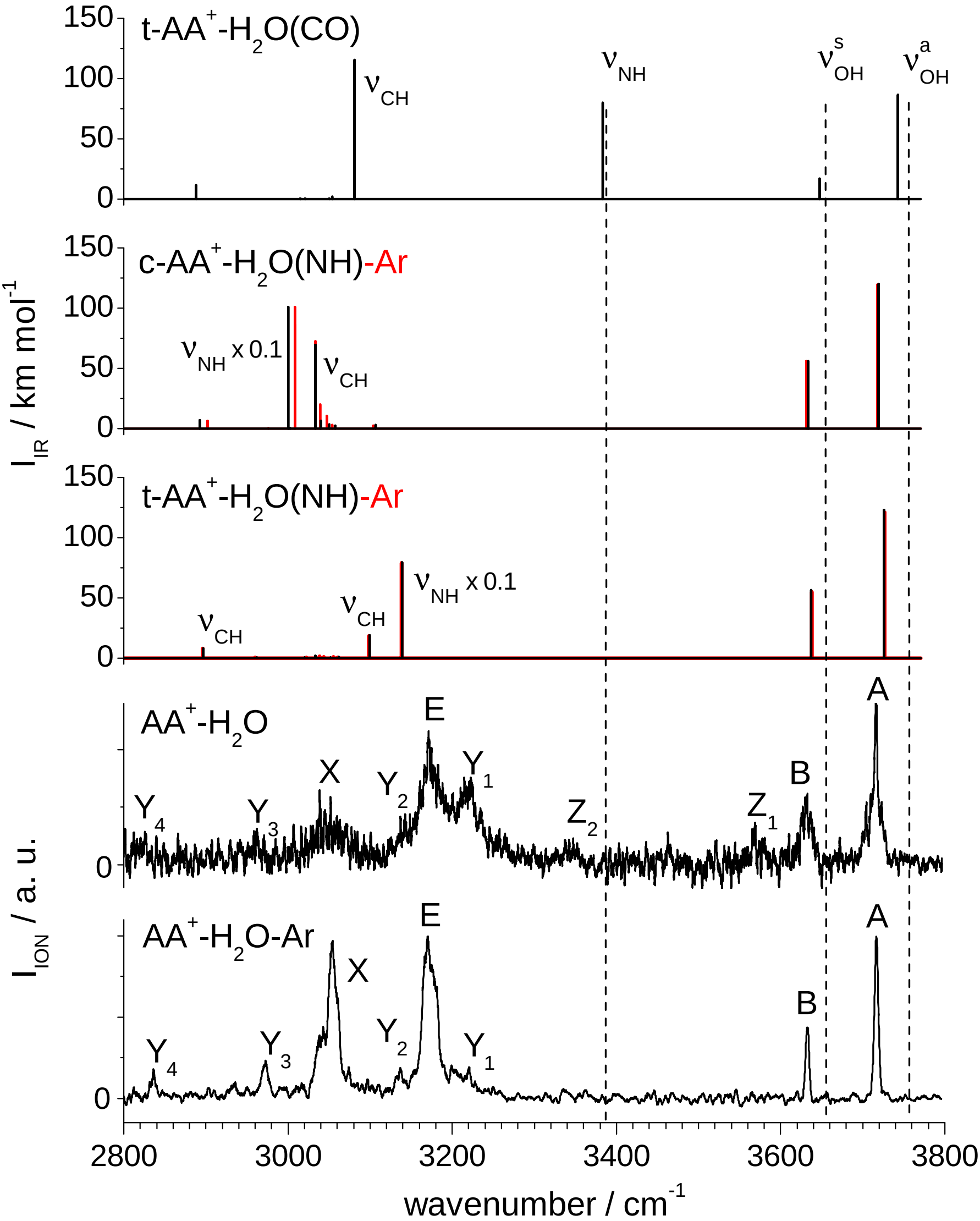
t-AA+-H2O(CO)
νCH
νNH
νOHs
νOHa
c-AA+-H2O(NH)-Ar
νNH x 0.1
νCH
t-AA+-H2O(NH)-Ar
νCH
νCH
νNH x 0.1
AA+-H2O
Y4
Y3
X
Y2
E
Y1
Z2
Z1
B
A
AA+-H2O-Ar
Y4
Y3
X
Y2
E
Y1
B
A
150
100
50
0
I_IR / km mol-1
I_ION / a. u.
2800
3000
3200
3400
3600
3800
wavenumber / cm-1

# FIGURE S4

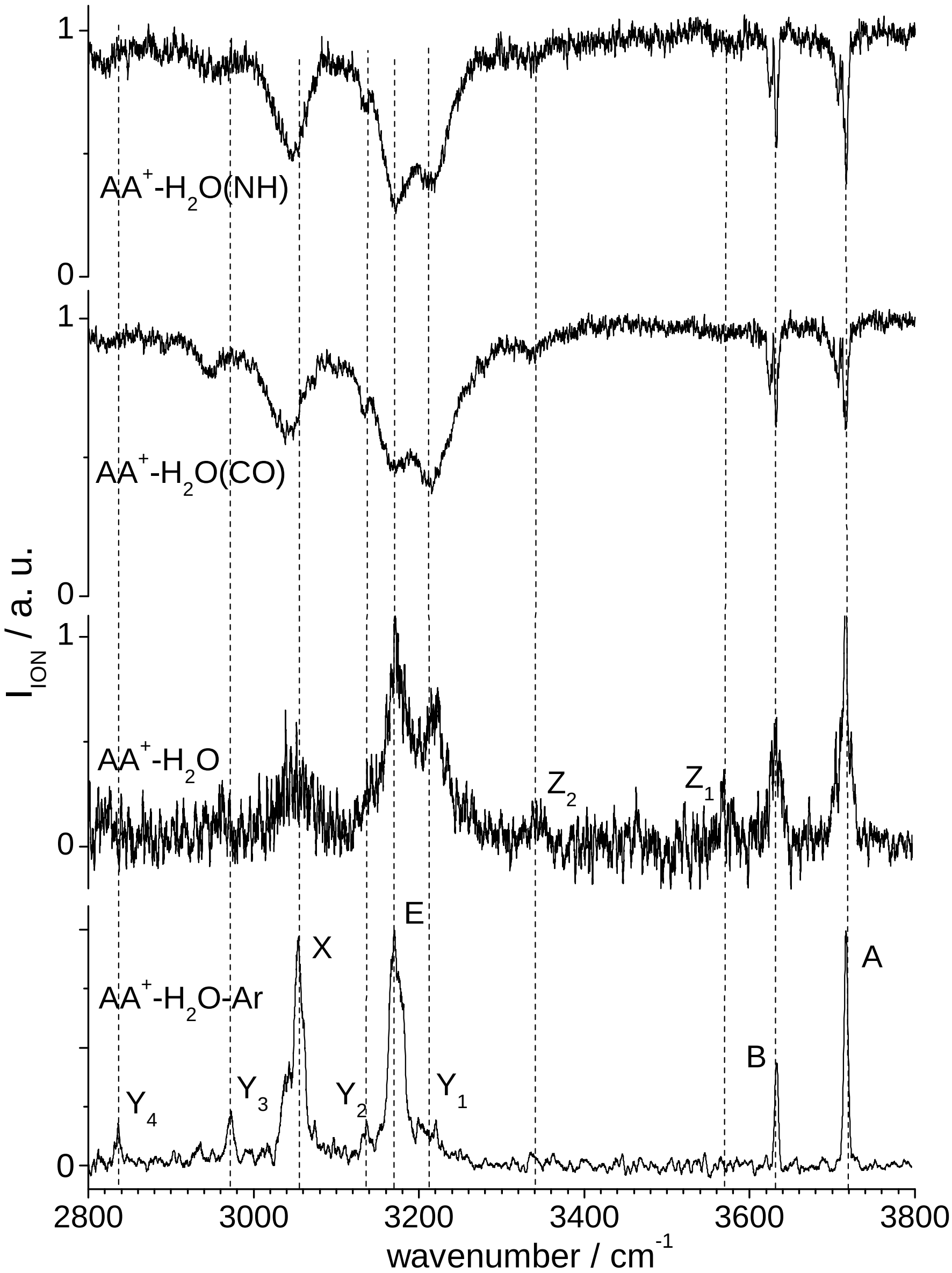
1
0
AA+-H2O(NH)
1
0
AA+-H2O(CO)
1
0
AA+-H2O
Z2
Z1
E
X
A
AA+-H2O-Ar
B
Y4
Y3
Y2
Y1
2800
3000
3200
3400
3600
3800
wavenumber / cm-1
I ION / a. u.

# FIGURE S5

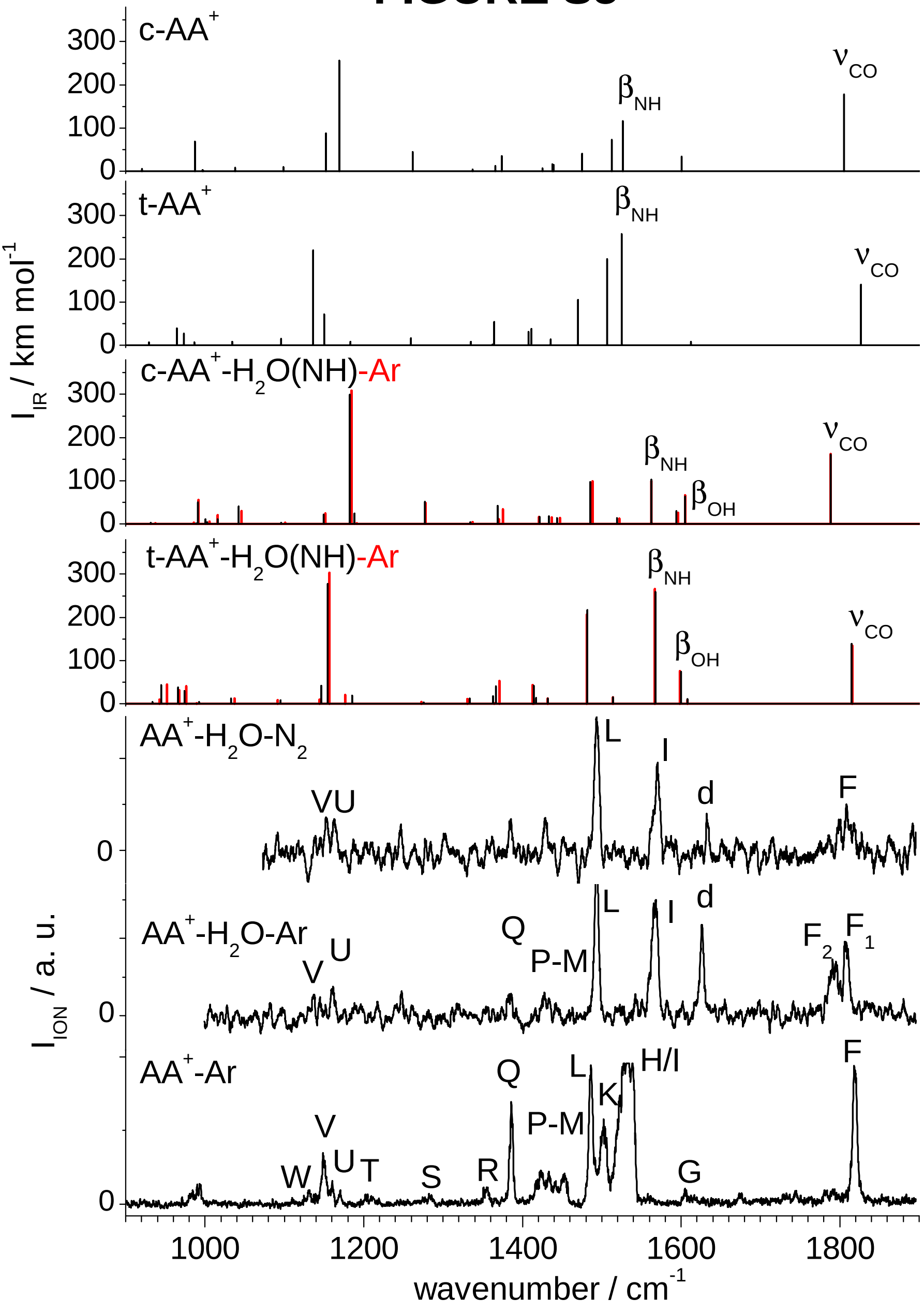
c-AA+
t-AA+
c-AA+-H2O(NH)-Ar
t-AA+-H2O(NH)-Ar
AA+-H2O-N2
AA+-H2O-Ar
AA+-Ar
βNH
νCO
βOH
I_IR / km mol-1
I_ION / a. u.
wavenumber / cm-1
1000
1200
1400
1600
1800

# FIGURE S6

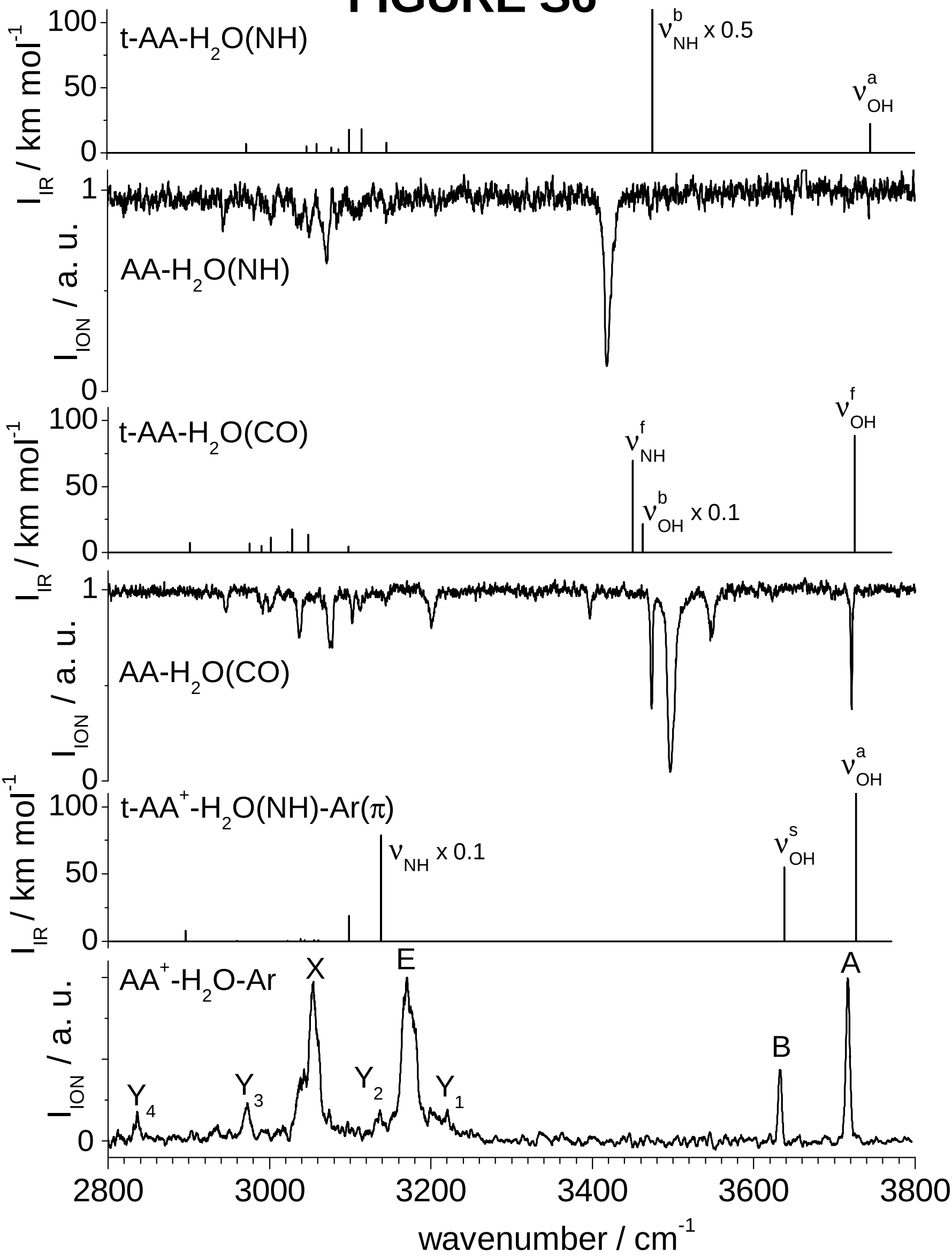
t-AA-H2O(NH)
$\nu_{NH}^{b}$ x 0.5
$\nu_{OH}^{a}$
I_IR / km mol^-1
I_ION / a. u.
AA-H2O(NH)
t-AA-H2O(CO)
$\nu_{NH}^{f}$
$\nu_{OH}^{f}$
$\nu_{OH}^{b}$ x 0.1
AA-H2O(CO)
$\nu_{OH}^{a}$
t-AA+-H2O(NH)-Ar(π)
$\nu_{NH}$ x 0.1
$\nu_{OH}^{s}$
AA+-H2O-Ar
X
E
A
B
Y4
Y3
Y2
Y1
2800
3000
3200
3400
3600
3800
wavenumber / cm^-1

# FIGURE S7

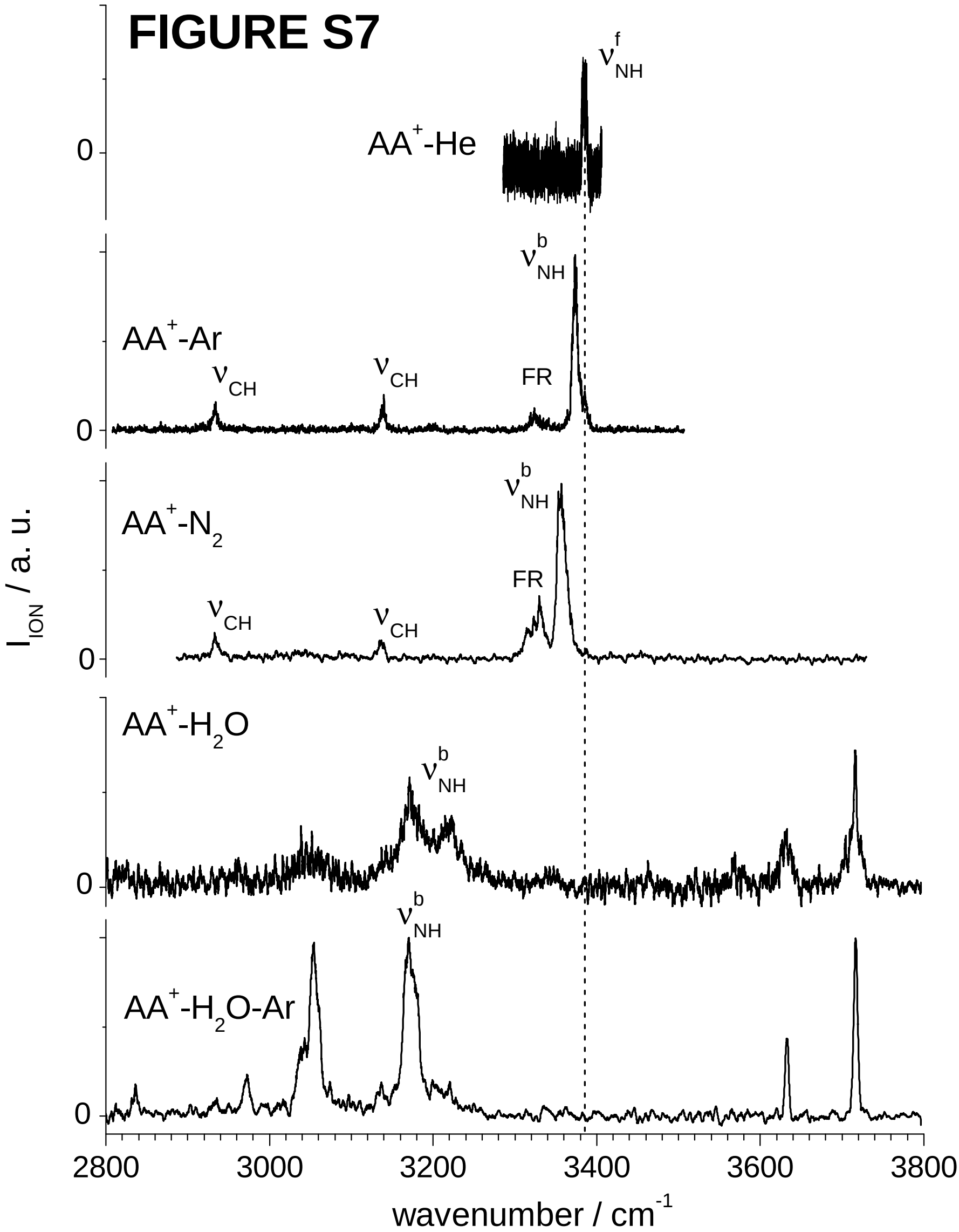
AA+-He
νNHf
AA+-Ar
νNHb
νCH
νCH
FR
AA+-N2
νNHb
νCH
νCH
FR
AA+-H2O
νNHb
AA+-H2O-Ar
νNHb
0
0
0
0
I ION / a. u.
2800
3000
3200
3400
3600
3800
wavenumber / cm-1

# FIGURE S8

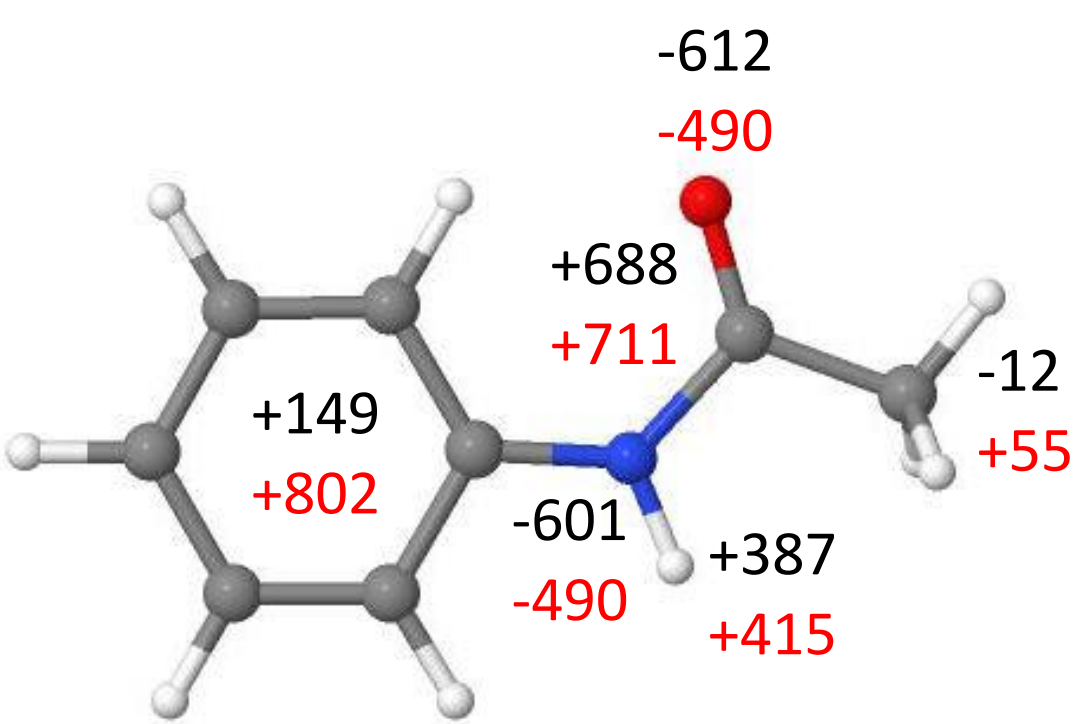


t-AA ($S_0$)

t-AA$^+$ ($D_0$)

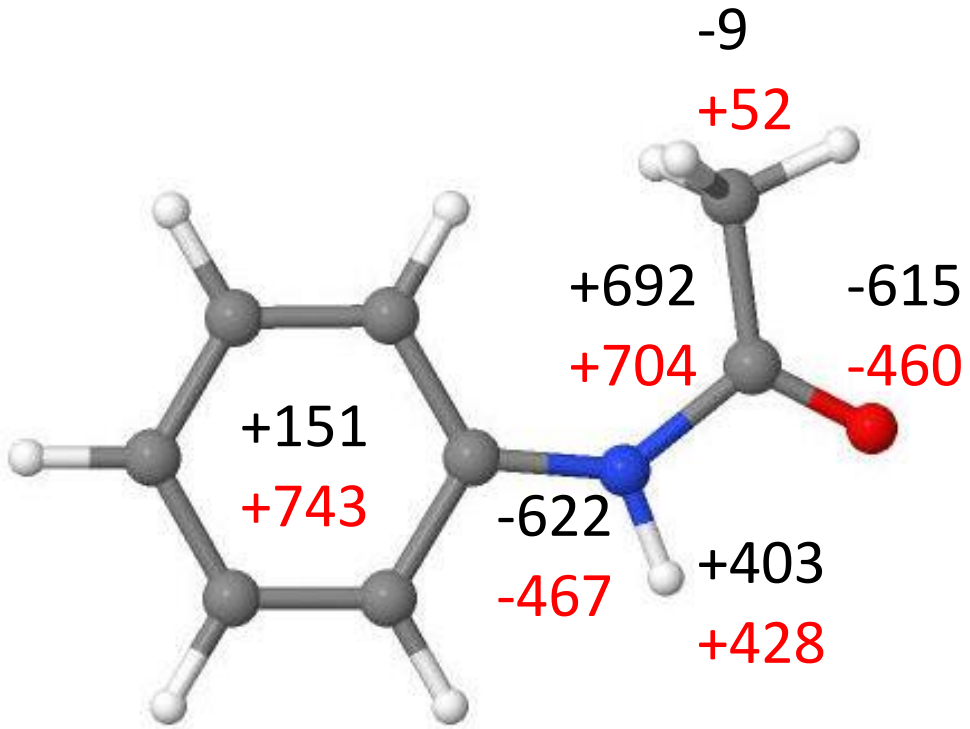


c-AA ($S_0$)

c-AA$^+$ ($D_0$)